Climate Dynamics (2025) 63:64
https://doi.org/10.1007/s00382-024-07536-0

ORIGINAL ARTICLE

Global estimation of terrestrial evapotranspiration based on the atmospheric water balance approach

Shasha Shang[1] · Ning Ma[2] · Gaofeng Zhu[3] · Kun Zhang[4] · Huiling Chen[5] · Zhenyu Zhang[6] · Xiaokang Liu[7] · Li Meng[1] · Yidong Wang[1,7]

Received: 9 August 2024 / Accepted: 1 December 2024

Abstract

Quantifying global terrestrial evapotranspiration (ET) relies on models with different levels of complexity. The water balance method offers a straightforward approach for benchmarking complex ET models, as evidenced by the widely-used terrestrial water-balance-based ET (ET_{TWB}) data. However, deriving ET_{TWB} must rely on ground-observed runoff data, which is not feasible for ungauged or poorly-gauged regions. In this context, the atmospheric water balance (AWB) method offers an alternative for estimating ET, which can be applied to the entire global land area. Nevertheless, the accuracy of the AWB approach in estimating global ET remains poorly understood. In this study, we generated monthly atmospheric water-balance-based ET (ET_{AWB}) globally from 1983 to 2020 at a 0.25° resolution using multi-source data. Validations against the annual ET_{TWB} of 56 large river basins suggest that ET_{AWB}, estimated using the moisture convergence and atmospheric water vapor from the fifth generation of European Center for Medium-Range Weather Forecasts Reanalysis (ERA5) and the precipitation from four observation-based products, is overall accurate. Specifically, the AWB method yields Nash–Sutcliffe efficiency coefficient (NSE), root mean square error (RMSE), and relative bias (RB) of 0.88, 89.5 mm $year^{-1}$, and 2%, respectively. These statistical metrics indicate that the AWB method is generally on par with current mainstream ET models. However, the AWB approach still has certain challenges in capturing the trend in ET. The ensemble mean ET_{AWB}, estimated using the moisture convergence and atmospheric water vapor from ERA5 and four precipitation datasets, yields a global-averaged value of 619 ± 8 mm $year^{-1}$ (excluding Antarctica) and shows an increase of 2.1% from 1983 to 2020, with a trend of 0.35 mm $year^{-1}$. Tropical regions exhibit pronounced interannual variability in ET_{AWB} due to the internal climate variability influencing precipitation and moisture convergence. The current AWB approach can potentially improve the understanding of regional and global ET processes, as it represents an independent approach to ET estimation, distinct from current remote sensing and land surface models.

Keywords Land evapotranspiration · Atmospheric water balance · Modeling and validations · Hydrological cycle

✉ Ning Ma
ningma@igsnrr.ac.cn

✉ Gaofeng Zhu
zhugf@lzu.edu.cn

[1] Tianjin Key Laboratory of Water Resources and Environment, Tianjin Normal University, Tianjin, China

[2] Key Laboratory of Water Cycle and Related Land Surface Processes, Institute of Geographic Sciences and Natural Resources Research, China Academy of Sciences, Beijing, China

[3] College of Earth and Environmental Sciences, Lanzhou University, Lanzhou, China

[4] School of Geospatial Engineering and Science, Sun Yat-Sen University, Zhuhai, China

[5] College of Geography and Environmental Sciences, Zhejiang Normal University, Jinhua, China

[6] Agroecosystem Sustainability Center, Institute for Sustainability, Energy, and Environment, University of Illinois Urbana-Champaign, Urbana, IL, USA

[7] School of Geographic and Environmental Sciences, Tianjin Normal University, Tianjin, China

Published online: 27 December 2024

1 Introduction

Evapotranspiration (ET) represents the total water vapor flux transferred from the land surface to the atmosphere, including evaporation from soil or water bodies, transpiration from vegetation, and evaporation of rainfall intercepted by the canopy. Globally, more than 60% of precipitation over land returns to the atmosphere (Ma et al. 2021; Oki and Kanae 2006), consuming approximately 50% of the net radiation available at the land surface (Trenberth et al. 2009; Wild et al. 2015), thereby linking the land and atmospheric branches of the hydrological cycle. Accordingly, ET is a crucial component of the Earth's system, affecting the exchange of water, carbon, and energy between the land surface and atmosphere (Fisher et al. 2017; Ma and Szilagyi 2019; Oki and Kanae 2006). Variation in ET is an important indicator of the response of hydrological cycle to global warming and influences terrestrial water availability (Ma and Zhang 2022; Seager et al. 2007; Sun et al. 2016, 2017; Zhang et al. 2023). However, compared to other components of the hydrological cycle, ET is poorly constrained (Jasechko et al. 2013; Liu et al. 2022; Syed et al. 2010; Volk et al. 2023; Yang et al. 2023). Therefore, accurate ET estimation is imperative for understanding the water cycle changes, weather, and climate dynamics (Trenberth et al. 2007; Zeng et al. 2017; Zhao et al. 2022).

Over the past few decades, significant progress has been made in estimating ET using ground-based observations and various models (Ma et al. 2015; Melo et al. 2021; Salazar-Martínez et al. 2022; Wang and Dickinson 2012). Among these methods, a range of measurement systems, including lysimeters, eddy covariance, Bowen ratio, and the eddy-covariance (EC) method, provide a direct measurement of ET (Allen et al. 2011) but are limited in a local scale and short time coverage, making them impractical at a global scale. Over recent years, a surge of global ET gridded products with different temporal and spatial resolutions have been developed from different types of models, including machine learning-based (Agrawal et al. 2022; Amani and Shafizadeh-Moghadam 2023; Jung et al. 2011), remote sensing-based (Fisher et al. 2020; Mu et al. 2007; Sun et al. 2023; K. Zhang et al. 2019; Zheng et al. 2022), reanalysis-based (Gelaro et al. 2017; Hersbach et al. 2020; Kobayashi et al. 2015), and land surface models (Cai et al. 2014; Li et al. 2022; Xia et al. 2012; Zhang et al. 2022), to complement in-situ observations. These ET models, varying in complexity, have significantly advanced our understanding of the ET process. However, these ET products inherently contain uncertainties stemming from the model structures or the forcing data. Previous studies have indicated that the spatial patterns of magnitude, trend, and variability globally differ significantly among various global ET gridded products (Ma et al. 2024; Tang et al. 2024). Reanalysis products usually have a coarse spatial resolution, along with inherent biases and uncertainties related to the assimilation process, especially in areas with sparse observations. Remote sensing-based models using satellite observations with advanced parameterizations of surface fluxes provide a promising approach to estimating ET, especially in poorly gauged basins. Nonetheless, spatial resolution mismatch between forcing data and vegetation data can introduce large uncertainties in ET estimation (Yang et al. 2013). Land surface models offer another approach for large-scale ET estimation, but the accuracy in soil parameters (e.g., soil texture, wilting point) largely impact the skill of land surface models in modeling ET (Li et al. 2019) constrains the accuracy of the ET estimates and usually results in a coarse spatial resolution (Long et al. 2014). Machine-learning-based datasets upscale flux-tower-based ET observations to regional or global scales using machine-learning algorithms with relatively higher accuracies, provided there are sufficient inputs of in-situ ET observations in the assimilation processes (Jung et al. 2019).

Owing to all the uncertainties across varying models, discrepancies between products impede the selection of the most appropriate ET data. Therefore, a systematic evaluation of the model results is necessary. EC observations, particularly from the FLUXNET networks worldwide (Pastorello et al. 2020), provide the most accurate data for evaluating estimated ET and have been extensively used to assess ET estimates from various models across different vegetation types (Li et al. 2021; Liu et al. 2023, 2013; Zhang et al. 2024). However, the temporal coverage of the EC observations is limited to post-2000 and sparse, especially in Africa, South America, and Asia (Pastorello et al. 2020). Additionally, issues such as the energy closure problem at some EC sites (Foken 2008) and spatial resolution mismatches remain intractable for evaluating ET products (Chu et al. 2021). Previous studies have suggested that empirical and statistical methods may be more accurate than complex physical and analytical methods for estimating ET (Kalma et al. 2008). This is because empirical and statistical methods are data-driven and independent of rigid theoretical model assumptions (Jung et al. 2010). Accordingly, water-balance-derived ET offers an alternative and effective methodology for evaluating modeled ET on larger scales (Builes-Jaramillo and Poveda 2018). The terrestrial water balance (TWB) approach is widely used to validate ET models (Jia et al. 2022; Szilagyi et al. 2024; Velpuri et al. 2013; Zhang et al. 2022), with ET calculated as the residual of precipitation minus the runoff and terrestrial water storage change at the basin scale (Rodell et al. 2004; Zeng et al. 2014). With the global availability

of terrestrial water storage from the Gravity Recovery and Climate Experiment (GRACE) with unprecedented accuracy since 2002, Ma et al., (2024) recently developed an observation-based terrestrial water balance-based ET (ET_{TWB}) dataset for 56 large river basins around the world, to providing a benchmarking tool for large-scale ET models. However, the TWB-estimated ET can only be used in gauged basins as it must rely on ground-observed runoff data. Additionally, there is a limitation on temporal coverage of ET_{TWB} because GRACE data only starts from 2002.

Apart from the TWB, the atmospheric water balance (AWB) offers an alternative framework to estimate ET, given that ET represents the total water vapor flux transported from the surface to the atmosphere, which is a crucial component in the atmospheric branch of the hydrological cycle. ET estimation based on AWB is derived from the residual of precipitation (P) minus atmospheric moisture convergence ($-\nabla \cdot Q$) and atmospheric water storage change $\left(\frac{\partial W}{\partial t}\right)$ (Oki et al. 1995). Compared to TWB, AWB do not need ground observed runoff in estimating ET. AWB relies on meteorological information, including winds and specific humidity, to calculate the atmospheric moisture convergence, which is typically sourced from reanalysis data. Meteorological observations used in reanalysis data are derived from radiosondes and are complemented by remote sensing techniques and atmospheric analysis models to achieve steady, time-continuous global coverage. Multiple reanalysis datasets have produced a coherent set of surface and upper-air meteorological data, utilizing modern satellite observations since 1979 or global radiosonde observations established in 1958, to understand the atmospheric hydrological cycle. Prominent reanalysis datasets include the National Aeronautics and Space Administration Modern-Era Retrospective-Analysis for Research and Applications v2 (MERRA2) (Gelaro et al. 2017), the Japanese Meteorological Agency55-year (JRA55) (Kobayashi et al. 2015), and the fifth generation of European Center for Medium-Range Weather Forecasts Reanalysis (ECMWF, ERA5) (Hersbach et al. 2020). As a crucial link between the terrestrial and atmospheric hydrological cycle, ET estimation from independent atmospheric data can potentially supplement water-balance-based ET, which is applicable anywhere and extends from the basin scale to the global scale. However, insight into the accuracy and spatial patterns of the global ET estimation based on AWB is still lacking. Given the inherent uncertainties in these reanalysis products related to different physical parameterizations, data assimilation procedures, and observational uncertainties (Miao et al. 2020; Ramon et al. 2019; Stopa 2018), it is necessary to evaluate the performance of different reanalysis in estimating ET using AWB approach to provide a reference for the community.

Therefore, this study aims to (1) estimate global ET on a monthly scale using the AWB approach; (2) determine whether the AWB approach improves upon current mainstream land ET products; and (3) quantify the global spatial and temporal variations in ET estimated by the AWB approach. The primary novelty of the present study is the new estimation of global ET by the AWB approach, which is different from previous land surface and remote sensing models.

2 Materials and methods

2.1 Atmospheric water balance

In this study, the atmospheric water-balance-based evapotranspiration (ET_{AWB}) was estimated using the atmospheric water balance equation (Oki et al. 1995):

$$ET_{AWB} = P - (-\nabla \cdot Q) - \frac{\partial W}{\partial t} \tag{1}$$

where P is the precipitation, $-\nabla \cdot Q$ is the mean convergence of the horizontal atmospheric water vapor fluxes, and $\frac{\partial W}{\partial t}$ represents the change of the atmospheric water storage. The vertically intergraded moisture convergence is calculated by:

$$-\nabla \cdot \mathrm{Q} = -\frac{1}{g}\nabla \cdot \int_0^{p_S} q\vec{V}dp \tag{2}$$

where p_s (Pa) is surface pressure, g (m s^{-2}) is gravitational acceleration, $\vec{V}$(m s^{-1}) is horizontal wind vector, and q (kg kg^{-1}) denotes the specific humidity.

Four precipitation datasets at a monthly scale used for ET_{AWB} estimates are consistent with those used to estimate terrestrial water-balance-based ET data (ET_{TWB}) for evaluation in this study (Ma et al. 2024). The corrected precipitation datasets include (1) Climatic Research Unit gridded Time series Version 4.06 at 0.5° resolution (Harris et al. 2020) (CRU, 1982–2020); (2) Global Precipitation Climatology Centre Full data Monthly Version 2022 at 0.25 resolution (Schneider et al., 2022) (GPCC, 1982–2020); (3) Global precipitation Climatology Project Version 3.2 Satellite-Gauge Combined Precipitation at 0.5° resolution (Huffman et al. 2023) (GPCP, 1983–2020); 4) Multi-Source Weighted Ensemble Precipitation Version 2.8 at 0.1° resolution (Beck et al. 2019) (MSWEP, 1982–2020). The monthly data for total column water vapor (precipitable water), specific humidity, winds from the surface to the top of the atmosphere, and vertically integrated moisture convergence are provided by three reanalysis datasets: (1) the fifth generation of European Center for Medium-Range Weather Forecasts

Reanalysis at 0.25° resolution (Hersbach et al. 2020) (ERA5, 1979-present); (2) Japanese 55-year Reanalysis at 1.25° resolution (Kobayashi et al. 2015) (JRA55, 1958-present); (3) Modern-Era Retrospective Analysis for Research and Applications at a native resolution of 0.5° latitude by 0.625° longitude (about 50 km in the latitude direction) (Bosilovich et al. 2015) (MERRA2, 1982-present). ERA5 and JRA55 datasets are available on a monthly scale whereas MERRA2 offers monthly means of data fields every six hours from 00:00 UTC. ERA5 is the fifth global atmospheric reanalysis product from ECMWF, succeeding ERA-Interim and earlier interactions, such as the First Global Atmospheric Research Program Global Experiment, ERA-15, and ERA-40. Compared to ERA-Interim, ERA5 has significantly improved pronouncedly in the observation system, assimilation scheme, and model algorithm (Hersbach et al. 2020). JRA55 is the third-generation reanalysis product, developed to address deficiencies in the first Japanese reanalysis project, the Japanese 25 year Reanalysis (JRA25), released by the JMA in 2010. JRA55 incorporates higher spatial resolution, a new radiation scheme, a simple inflation factor scheme, and bias correction, providing a long-term comprehensive atmospheric dataset. MERRA2 replaces the original MERRA dataset created by NASA. In MERRA2, the atmospheric assimilation system was upgraded to assimilate newer satellite observations, and a newer Goddard Earth Observing System Model, Version 5 (GEOS5) system was employed. All precipitation and reanalysis data were interpolated to a 0.25° resolution using the nearest neighbor method. ET_{AWB} was calculated at a 0.25° resolution on a monthly scale, corresponding to the periods of precipitation data.

2.2 Terrestrial water-balanced ET data

Terrestrial water-balance-based evapotranspiration (ET_{TWB}) data for 56 large ($> 10^5$ km^2) river basins worldwide derived from Ma et al., (2024) are used for evaluation in this study. This dataset was generated using a Bayesian-based three-cornered hat method from 12 annual ET_{TWB} time series, which derived from the observed runoff, four different precipitation data sources, and three types of terrestrial water storage change estimates. The accuracy of the ET_{TWB} dataset from Ma et al., (2024) was significantly improved by using bias-corrected precipitation. Using multiple precipitation and terrestrial water storage change estimates further benefits its applicability in large-scale ET model revaluations. The distribution of 56 river basins is shown in Fig. 1, and basic information about these basins is summarized in Supplementary Table 1. Further details on this dataset can be found in Ma et al., (2024).

2.3 Long-term gridded global ET products

In this study, we selected three typical long-term gridded global ET products for inter-comparison, which include (1) The Global Land Evaporation Amsterdam Model (GLEAM) Version 3.6a (Martens et al. 2017), which is a remote sensing-based models; (2) The Simple Terrestrial Hydrosphere (SITH) model (Zhang et al. 2024), a data-driven diagnostic model developed based on the groundwater-soil–plant-atmosphere continuum by Zhu et al., (2019) and Zhang et al., (2022); and (3) The ET from the ERA5 reanalysis (Hersbach et al. 2020), which is essentially the output for a Hydrology-Tiled ECMWF Scheme for Surface Exchange over Land. All three ET products cover the period of 1982–2020 with a spatial resolution of 0.25°. These three ET products were selected for long-term coverage that aligns with the period of the ET_{AWB} dataset.

2.4 Evaluation metrics

The ET_{AWB} dataset is compared with ET_{TWB} at 56 basins as well as with three long-term global ET datasets at the basin scale, global scale, and various climate zones. Evaluation metrics include root mean square error (RMSE), Nash–Sutcliffe efficiency coefficient (NSE), correlation coefficient (R), and relative bias (RB). The significance of the ET trend is tested using Student's *t*-test.

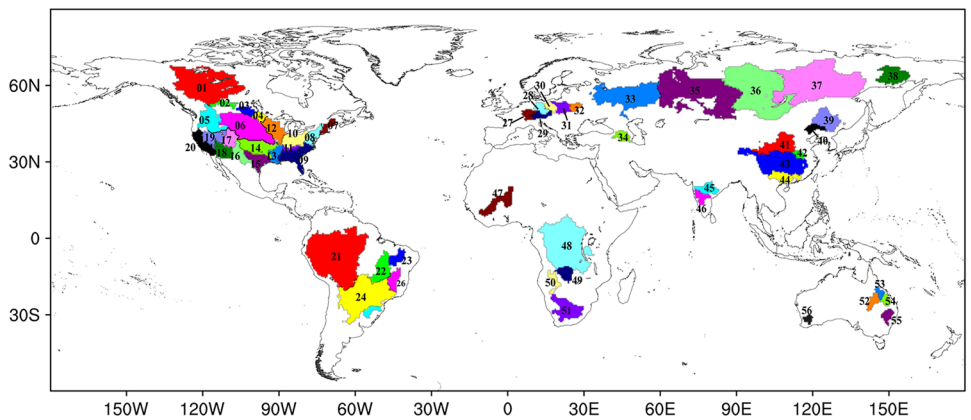

Fig. 1 Spatial distribution of 56 river basins for the ET_{TWB} data used in this study (Modified from Ma et al. 2024). The numbers correspond to the IDs in Table S1

2.5 Uncertainty calculation

The uncertainty of the ET_{AWB} is calculated by the uncertainties in each variable of Eq. (1) which assumes the errors in them are independent (Dingman, 2015).

$$\delta_{ET_{AWB}} = \sqrt{\delta_P^2 + \delta_Q^2 + \delta_{\frac{\partial W}{\partial t}}^2} \quad (3)$$

where δ represents the uncertainty of the variable specified by the subscript. The δ_P, δ_Q and $\delta_{\frac{\partial W}{\partial t}}$ are calculated as the standard deviation across three precipitation products and four reanalysis datasets.

3 Results

3.1 Evaluation of the ET_{AWB} estimated using precipitation, moisture convergence, and atmospheric water vapor from multiple data sources

The ET_{AWB} was estimated using moisture convergence and atmospheric water vapor from three reanalysis datasets (ERA5, JRA55, and MERRA2), and precipitation from four observe-based precipitation datasets (CRU, GPCC, GPCP, and MSWEP). Figure 2 illustrates the spatial distribution of the basin-averaged multi-year mean annual ET_{AWB} from various data sources relative to the ET_{TWB} in 56 river basins, along with the corresponding regression plot. The results reveal minimal spatial difference in the 12 multi-year mean ET_{AWB} across different precipitation datasets, but significant differences among different reanalysis data. Annual mean ET values derived by the moisture convergence and atmospheric water vapor from ERA5 exhibit particularly high accuracy (NSE ≥ 0.86, RMSE ≤ 97.5 mm year^{-1}, R ≥ 0.947, and RB ≤ 6.2%) (Figs. 2a ~ d). The proportion of relative errors within ± 10% is at least 40% out of 56 basins. Annual mean ET_{AWB} values derived from JRA55 and MERRA2 exhibit relatively poor performance, tending to significantly overestimate ET_{TWB} in most basins. RMSE values reach up to 350 mm year^{-1}, and NSE values are even negative. The relative errors exceed ± 20% in more than 40 of 56 basins. The ET_{AWB} estimates using moisture convergence and atmospheric water vapor from JRA55 and MERRA2 relative to ET_{TWB} exhibit a similar spatial distribution, with overestimation exceeding 60% in regions such as eastern Siberia, including the Yenisy (Basin #36), Lena (Basin #37), and Kolyma basins (Basin #10); the United States, including the Columbia (Basin #05), Rio Grande (Basin #16), Upper Colorado (Basin #17), Lower Colorado (Basin #18), Great Basin (Basin #19) and California (Basin #20) basins; and

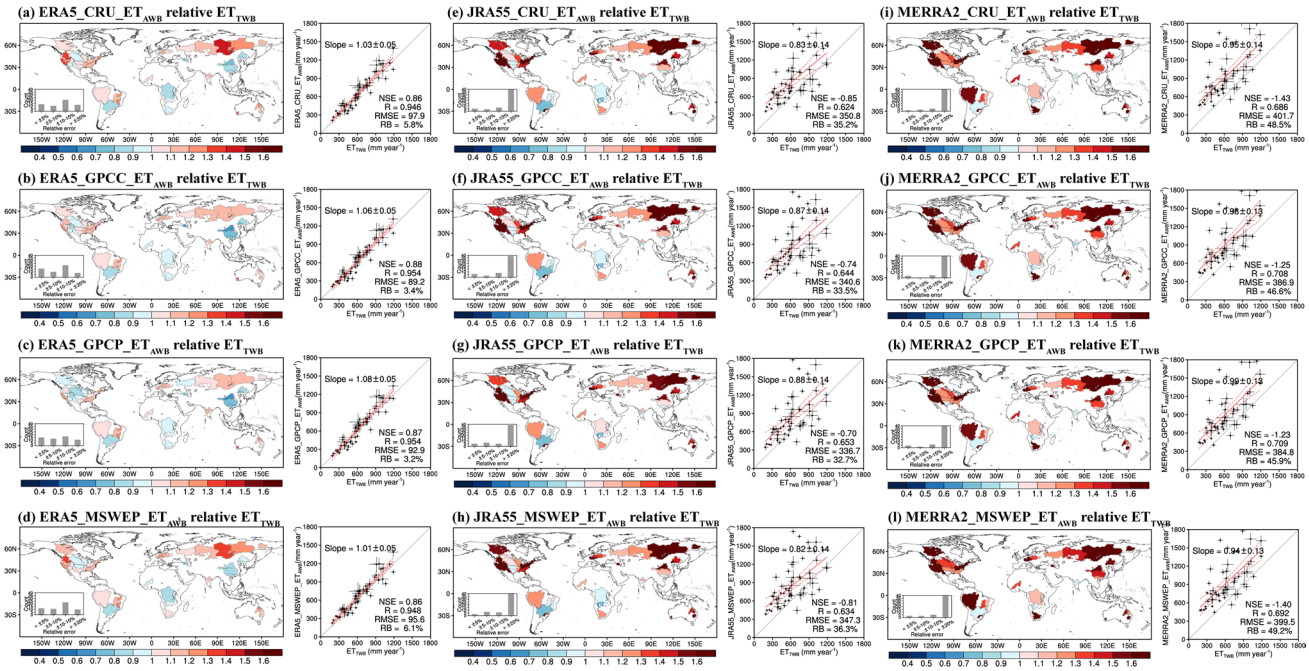

Fig. 2 Evaluations of ET_{AWB} based on multiple reanalysis and precipitation datasets against the terrestrial water-balanced ET_{TWB} for 56 basins from 1983 to 2016. The inset in the spatial distribution plot shows the number of basins within specified relative error ranges. The length of the whiskers denotes the standard deviation of the basin-averaged annual ET during the period 1983–2016. NSE refers to Nash–Sutcliffe efficiency. The strips around the least-squares-fitted red line, with its specified slope indicate the 95% confidence intervals. RMSE is the root mean square error in mm year^{-1}

coastal regions in eastern United States, including New England (Basin #07) and the Mid-Atlantic (Basin #08) region as well as in the Mackenzie Basin (Basin #01).

The uncertainty of monthly precipitation, moisture convergence, change of the atmospheric water vapor storage, and the ET_{AWB} are shown in Fig. 3. The uncertainty of precipitation mainly occurs in high-precipitation areas including the Maritime Continent, Amazon, and Congo Basin, which shows the largest difference across different precipitation data. It is shown that the uncertainty of the atmospheric water storage change is less than 2 mm month^{-1} since changes in atmospheric water storage in the AWB are negligible over long timescales (Dominguez et al. 2006; Rasmusson 1968). The spatial pattern of the uncertainty for ET_{AWB} is similar to that of the atmospheric moisture convergence with larger uncertainties in high-altitude regions, including the Rocky Mountains, the Andes Mountains, the East Africa Plateau, the Tibetan Plateau, and the Maritime Continent near the equator. The result indicates that the uncertainties of ET_{AWB} stem primarily from the uncertainty in moisture convergence.

To further investigate the reasons for the significant overestimation and discrepancies in ET_{AWB} values that use the moisture convergence from JRA55 and MERRA2, Fig. 4 illustrates the spatial distribution of atmospheric moisture convergence from JRA55, MERRA2, and ERA5. The spatial patterns of multi-year mean atmospheric moisture convergence from ERA5, JRA55, and MERRA2 are generally consistent, all capturing significant convergence in the Intertropical Convergence Zone (ITCZ). The differences mainly occurred in western United States and eastern Siberia, where JRA55 and MERRA2 show moisture divergence, while ERA5 indicates moisture convergence (Fig. 4 and Figure S1). The differences in moisture convergence patterns are consistent with the discrepancies in ET_{AWB} estimates (Fig. 2). Figure S2 also shows the distributions of multi-year mean precipitation values across the four products are similar, minor differences (no more than $\pm$ 10 mm month^{-1}) are observed, except in Greenland (Figures S2 and S3). The results suggest that the significant overestimation of the ET_{AWB} in some basins derived from the JRA55 and MERRA2 may be attributed to the bias in moisture convergence. Caution is advised when using winds and specific humidity from JRA55 and MERRA2 to calculate atmospheric moisture convergence for analyzing related atmospheric circulations in these regions. Overall, the evaluation of ET_{AWB} estimated using multiple data sources against ET_{TWB} superior performance of the moisture convergence and atmospheric water vapor from the ERA5 reanalysis compared to JRA55 and MERRA2, regardless of precipitation data.

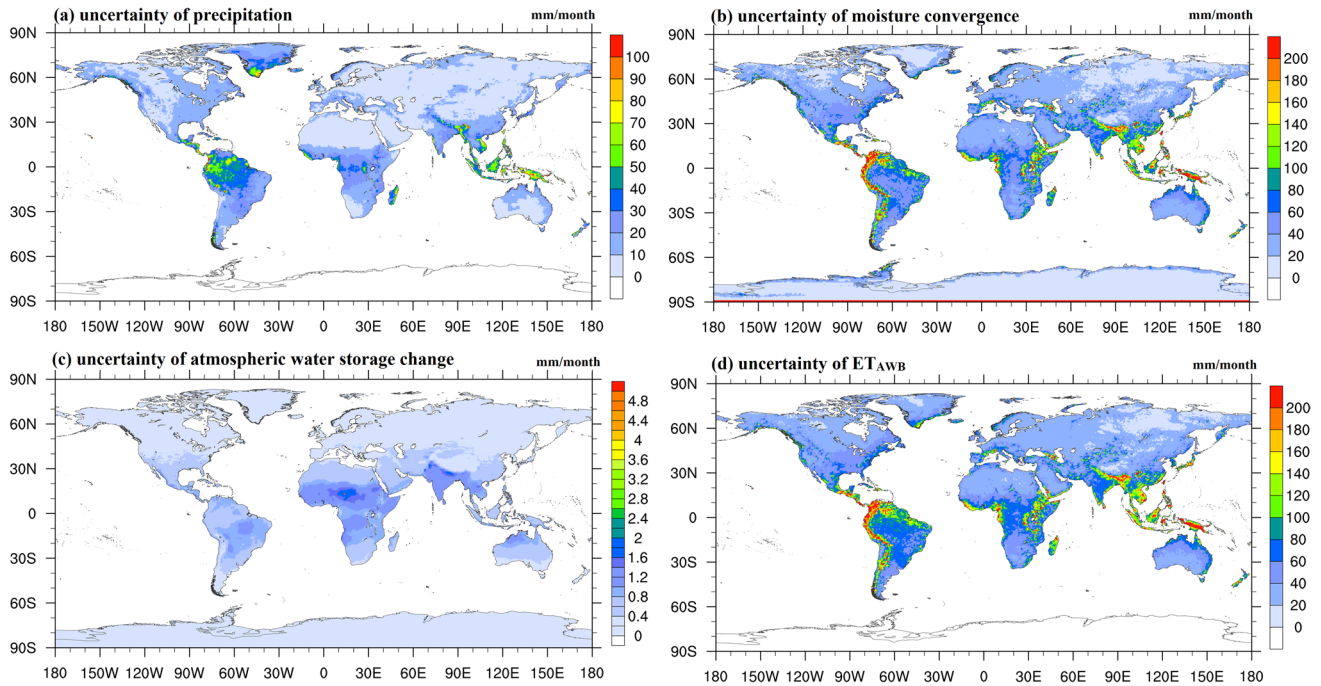

Fig. 3 Spatial distribution of the multi-year mean monthly uncertainty in **a** precipitation; **b** moisture convergence; **c** atmospheric water storage change; and **d** ET_{AWB} globally

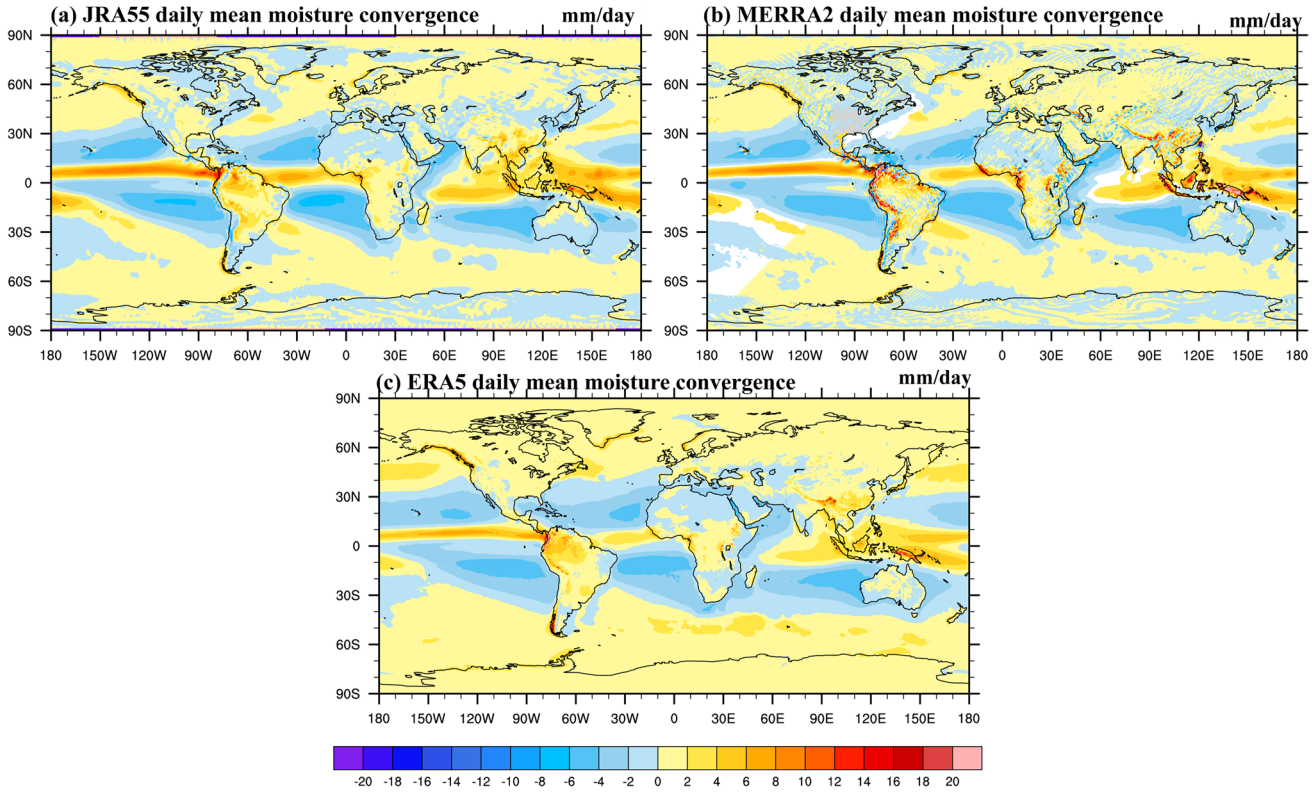

Fig. 4 The spatial distribution of multi-year mean moisture convergence from **a** JRA55, **b** MERRA2, and **c** ERA5

3.2 Evaluation of the ensemble mean ET_{AWB} against ET_{TWB}

Given the biases of moisture convergence in JRA55 and MERRA2 reanalysis, only the total column water vapor and moisture convergence from ERA5 were used to calculate ET_{AWB}. Additionally, due to minimal differences among the various precipitation datasets, we merged four ET_{AWB} time series derived from the ERA5's total column water vapor and moisture convergence, and the four precipitation datasets by calculating their arithmetic average to obtain the ensemble mean ET_{AWB}. In the subsequent sections, we focus solely on this ensemble mean ET_{AWB}. For a comparison purpose, we also included three mainstream long-term global ET products to see if ET_{AWB} improves upon them.

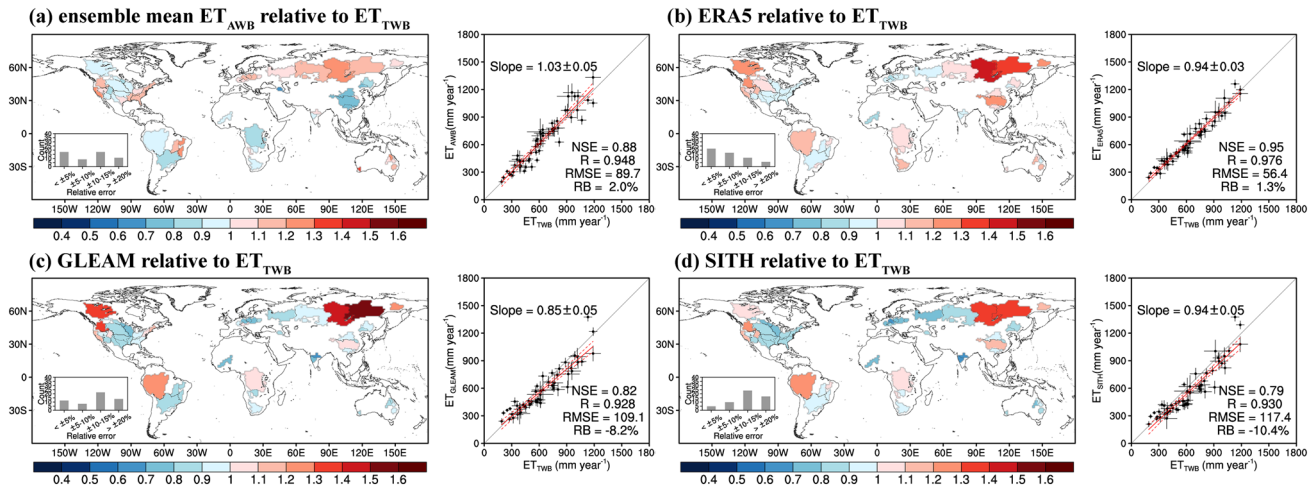

Fig. 5 Same as Fig. 2 but for the ensemble mean ET_{AWB}, ERA5, GLEAM, and SITH

We first evaluate the accuracy of ET_{AWB} in the ET magnitude against the ET_{TWB}. As seen from Fig. 5a, the AWB approach is overall satisfactory in depicting the ET magnitude with NSE, RB, and RMSE values of 0.88, 2%, and 89.7 mm $year^{-1}$, respectively. While the statistical metrics of ET_{AWB} are somewhat worse than the ERA5, they are much better than two diagnostic remote sensing models—GLEAM and SITH. In particular, the RB of ET_{AWB} is solely 2%, which is very close to ERA5 with 1.8%, and both are much less than those from GLEAM and SITH (− 8.2% and − 10.4%). This indicates that the AWB approach substantially reduces the error in the ET estimates compared to the modeled ET.

From a spatial perspective, ET_{AWB} slightly underestimates ET values in basins in the central United States and low- and mid-latitudes by 10–30%, but overestimates ET in Northern Eurasia basins by 10–20%. However, ERA5, GLEAM, and SITH significantly overestimate ET values by more than 50% over two Arctic basins in eastern Siberia including Yenisy (Basin #36) and Lena (Basin #37). The larger errors in these basins may be attributed to the freeze–thaw processes at high latitudes, which directly affect soil water content, and in turn, influence the ET process (Niu & Yang, 2006). The current process-based ET models do not effectively incorporate the freeze–thaw process with available calibration data (e.g., subsurface ice), making accurate ET estimation in these specific regions particularly challenging. Additionally, the relative errors of ET_{AWB} are within ± 10% in more than 30 out of 56 basins, which is also superior to GLEAM and SITH, both have no more than 20 basins with a relative bias under 10%.

We further evaluated the skills of the AWB approach in depicting the trends in annual ET rates from 1983 to 2016 (Fig. 6). The evaluation indicates that, despite its accuracy in specific regions such as the Congo Basin (Basin #49, 50), Amazon (Basin #21), and western Europe (Basin #28, 30), the performance of ET_{AWB} in describing the ET trends is inferior compared to the other three ET products. GLEAM demonstrates the highest skill in capturing ET trends, with an NSE value of 0.4, an RMSE value of 1.2, and a slope value of 0.59. However, the AWB approach, ERA5, and SITH similarly show negative NSE values when evaluating

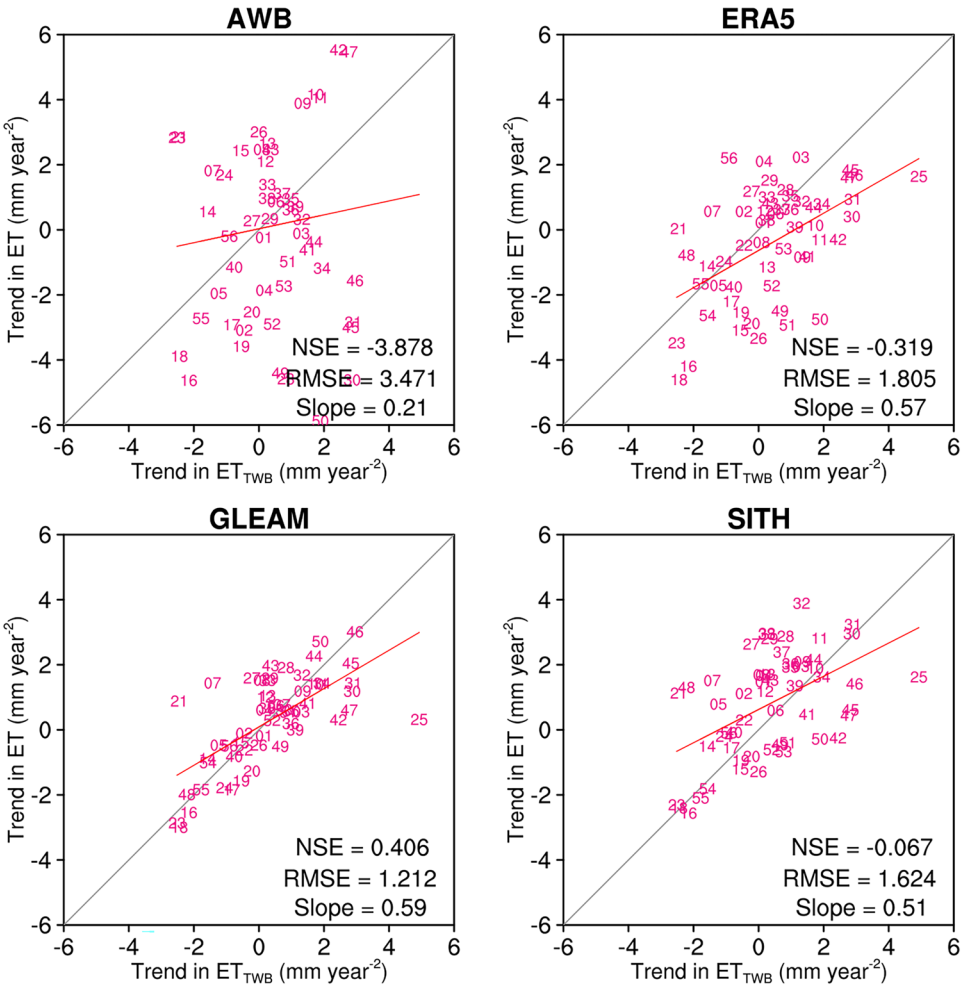

Fig. 6 Evaluation of the trends (1983–2016) in the annual ET estimates of ERA5, GLEAM, SITH, and ensemble mean ET_{AWB} against the ET_{TWB} values of 56 river basins globally. The numbers represent the basin ID in Fig. 1 and Table S1. RMSE is in mm $year^{-2}$. The red line is the least-square-fitted first-order polynomial with its slope

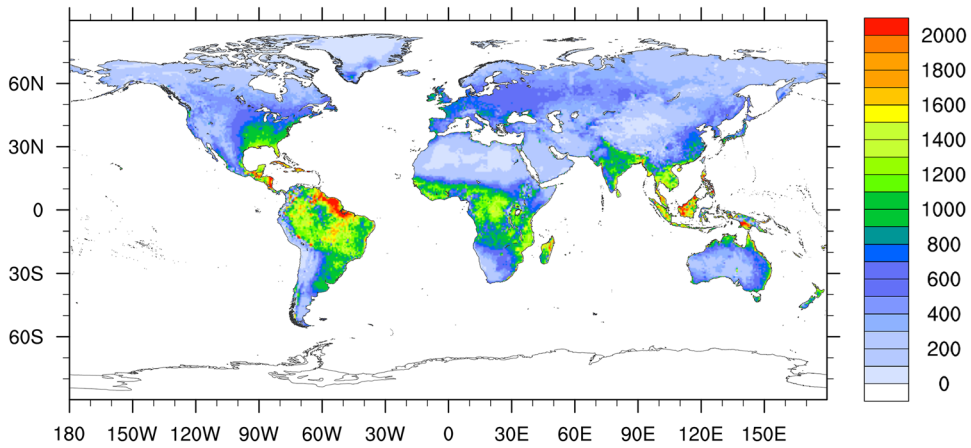

Fig. 7 Spatial pattern of the multi-year mean annual ET from 1983 to 2020 from the ensemble ET_{AWB} (mm $year^{-1}$)

against the trends in ET_{TWB}. These results suggest that caution should be exercised when using the AWB approach to derive the trends in ET on a global scale.

3.3 Spatial and temporal variations in ET estimated by the AWB approach

Figure 7 presents the global distribution of the multi-year (1983–2020) mean annual ET estimated using the AWB approach. ET_{AWB} shows the highest ET values in tropical regions (Amazon, Congo Basin, Maritime Continent, and Southeast Asia) around the equator ($\geq$ 1200 mm $year^{-1}$), and intermediate ET values in mid-latitude humid regions (600–1200 mm $year^{-1}$). The lowest ET values are observed in permanent ice- and snow-covered regions of Greenland, desert, and arid regions (e.g., Sahara and central Asia) ($\leq$ 200 mm $year^{-1}$). Low ET values also occur in high altitudes regions in mid- and low-latitudes, such as the Tibetan Plateau in Asia and the Rocky Mountains in South America. Because there is no precipitation data for Antarctica from CRU and GPCC (Figure S2), the ET_{AWB} is missing in Antarctica. Overall, the geographical distribution of annual ET values estimated by the AWB approach is in close agreement with the long-term mainstream ET products as illustrated in Figure S4 and other state-of-the-art global ET estimates derived using different methods (e.g., Ma et al. 2021; Mu et al. 2007; Tang et al. 2024; Zeng et al. 2014).

Figure 8 illustrates the annual anomalies of ET_{AWB}, as well as the other three products over the period 1983–2020. It is shown that the interannual variations are generally within the range of the three long-term mainstream ET products, though there are anomalously low values in 1986 and 1987, and anomalously high values in 1998 and 2000. The global multi-year annual mean ET values (excluding the Antarctica) estimated by AWB, ERA5, GLEAM, and SITH is 619 $\pm$ 8 mm $year^{-1}$ (mean $\pm$ standard

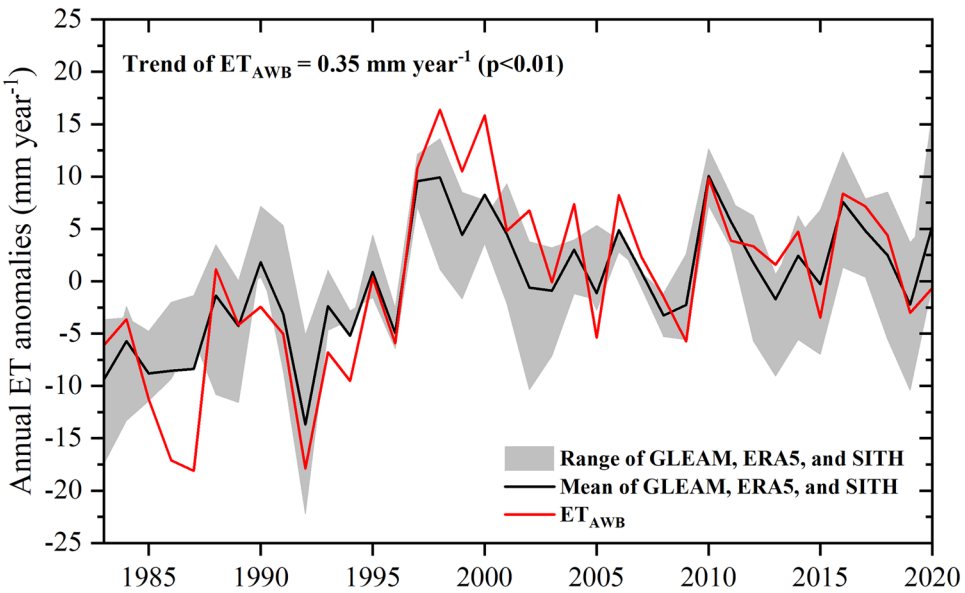

Fig. 8 Annual anomalies of global averaged ET (excluding Antarctica) estimated from the AWB approach during 1983–2020. The mean value plus the range of GLEAM, ERA5, and SITH are also specified (black solid line and gray shadow)

deviation), 582 ± 5.7 mm year^{-1}, 560 ± 6 mm year^{-1}, and 499 ± 8.4 mm year^{-1}, respectively. The magnitude of the global mean annual ET_{AWB} is within the range of the global average of 25 ET products and is close to their ensemble mean (628 ± 44 mm year^{-1}) (Tang et al. 2024). The trend of the annual ET_{AWB} from1983 to 2020 is 0.35 mm year^{-1}, indicating an increase of 2.1% over the last 38 years, which is generally consistent with previous studies (Kim et al. 2021; Ma et al. 2021) and also the ensemble mean of the other three products shown here (Fig. 8).

Figure 9 shows the spatial patterns of the linear trends in annual ET estimated by AWB across the world**.** In the Northern Hemisphere, annual ET_{AWB} shows significant increasing trends in the eastern United States, Sahara, southeastern China, and the Indochina Peninsula. However, significant decreasing trends occur in the western and northwestern United States. Significant increasing trends are also observed near the equator, including the Amazon, the Congo Basin, and the Maritime Continent. In the Southern Hemisphere, significant decreasing trends are observed in the southern section of the Cordillera, South Africa, and the central Australian Plains. Indeed, there are some discrepancies in the distribution of linear trends among ET_{AWB} and the other three products on a global scale (Figure S5). This was evidenced in the comparison of spatial–temporal patterns for 25 global ET products by Tang et al., (2024), which indicates that the trends from different global ET products are not uniform on a global scale. Nevertheless, ET_{AWB} offers a reference for the global ET spatial trends from the perspective of atmospheric water balance.

Figure 10 presents the spatial pattern of interannual variability in estimated annual ET from AWB. The interannual variability of ET_{AWB} is notably stronger in tropical regions (≥ 200 mm year^{-1}), such as the Amazon, Congo Basin, Southeastern Asia, and the Maritime Continents. Intermediate interannual variability occurred in the eastern United States, South Africa, and southwestern China. The interannual variability of ET values tends to decrease with increasing latitudes in the Northern Hemisphere. The weakest interannual variability occurs in the Sahara and northern Greenland. The extremely high interannual variability in ET_{AWB} values in tropical regions may be attributed to the influence of independent variables, including precipitation and atmospheric moisture convergence, on its estimates (Figure S6) (Yeh and Famiglietti 2008). Because precipitation and moisture convergence are highly influenced by

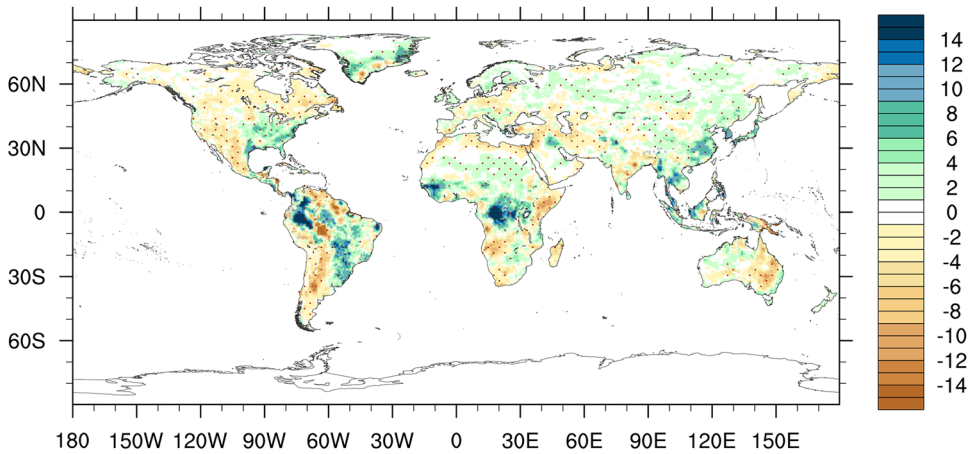

Fig. 9 Spatial pattern of the linear trends in ensemble ET_{AWB} (mm year^{-1}). Dotted regions indicate that linear trends are statistically significant at the 95% confidence level

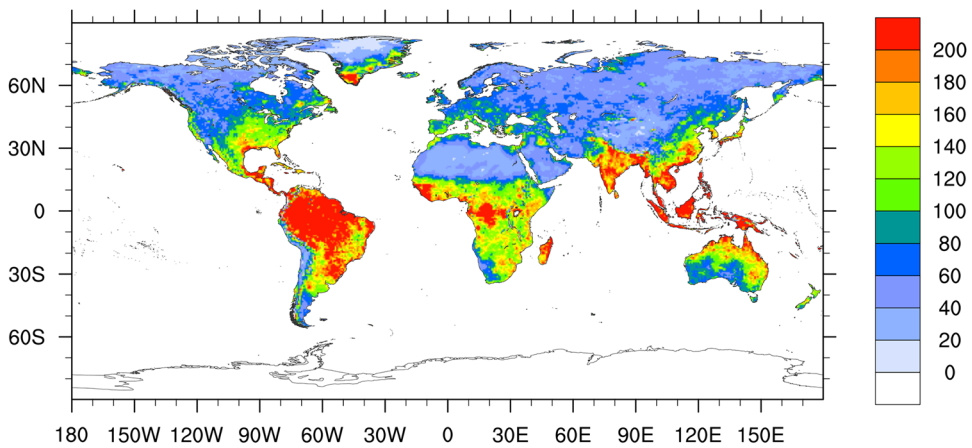

Fig. 10 Spatial distribution of interannual variability (standard deviation) of the ensemble mean ET_{AWB} (mm year^{-1})

atmospheric circulation and internal climate variability, such as the El Niño-Southern Oscillation (ENSO), the North Atlantic Oscillation (NAO), and the Indian Ocean Dipole (IOD) (Mo 2010; Shang et al. 2021; Yan et al. 2020; Yang et al. 2021). This limitation arises from the calculation of ET_{AWB} solely from the atmospheric perspective, which neglects the influence of land surface processes. Yeh and Famiglietti, (2008) have demonstrated that the AWB approach using reanalysis data has the potential to estimate climatological ET variations but may not be suitable for diagnosing the interannual variability.

To illustrate the characteristics of ET_{AWB} under various climate conditions, global land areas were categorized into five main types based on the Köppen climate system: tropical, dryland, temperate, continental, and polar and alpine zones (Beck et al., 2018) (Figure S7). The multi-year mean annual and seasonal cycles of ET values estimated by AWB are shown in Fig. 11. The multi-year mean annual ET values for the tropical, temperate, continental, dryland, and polar-alpine zones are 1295 ± 38 mm year^{-1}, 691 ± 11 mm year^{-1}, 80 ± 7 mm year^{-1}, 447 ± 16 mm year^{-1}, 168 ± 18 mm year^{-1}, respectively (Fig. 11a). The magnitudes of ET in the continental and dryland zones are comparable. For the seasonal cycle of different climate zones estimated by ET_{AWB}, minimal seasonality is shown in the tropical, temperate, dryland, and polar-alpine zones. The tropical zone exhibits the highest magnitude (about 12 mm month^{-1}) each month, which is characterized by hot and rainy conditions throughout the whole year. In contrast, the dryland and polar-alpine zones are characterized by consistently low ET all year. The temperate zone is characterized by consistent precipitation and temperature throughout the year, also with relatively minor variations in ET across months. The continental zone, located entirely in the Northern Hemisphere, exhibits significant seasonal variations in ET, with high values in summer (June, July, and August) and low values in winter (November, December, and January). Overall, ET_{AWB} effectively captures the climate characteristics of various climate zones.

4 Discussion

4.1 Advantages and disadvantages of the AWB approach in global ET estimation

The atmospheric water balance (AWB) offers an effective framework for estimating ET using independent atmospheric data, without the need for input parameters related to soil and vegetation, thereby complementing water-balance-based ET estimates and enriching existing ET datasets. From a spatial perspective, reanalysis datasets combine in situ measurements with state-of-the-art numerical models to provide the best possible analysis of the atmosphere. This offers a comprehensive record of global atmospheric circulations (Berrisford et al. 2011). By employing more refined reanalysis with increased ground observations and advanced assimilation methods, such as the ERA5, the AWB approach provides a direct method to estimate ET on regional to global scales. In contrast, ET estimates derived from the TWB approach are limited in basin scales (Ramillien et al. 2006; Zeng et al. 2014). From a temporal perspective, modern satellite observations since 1979, combined with global radiosonde observations since 1958 and atmospheric analyzing models, produce reanalysis data that is steady and time-continuous from 1979 to the present. This enables the long-term time series ET estimates based on the AWB. However, TWB-based ET estimates are generally restricted to

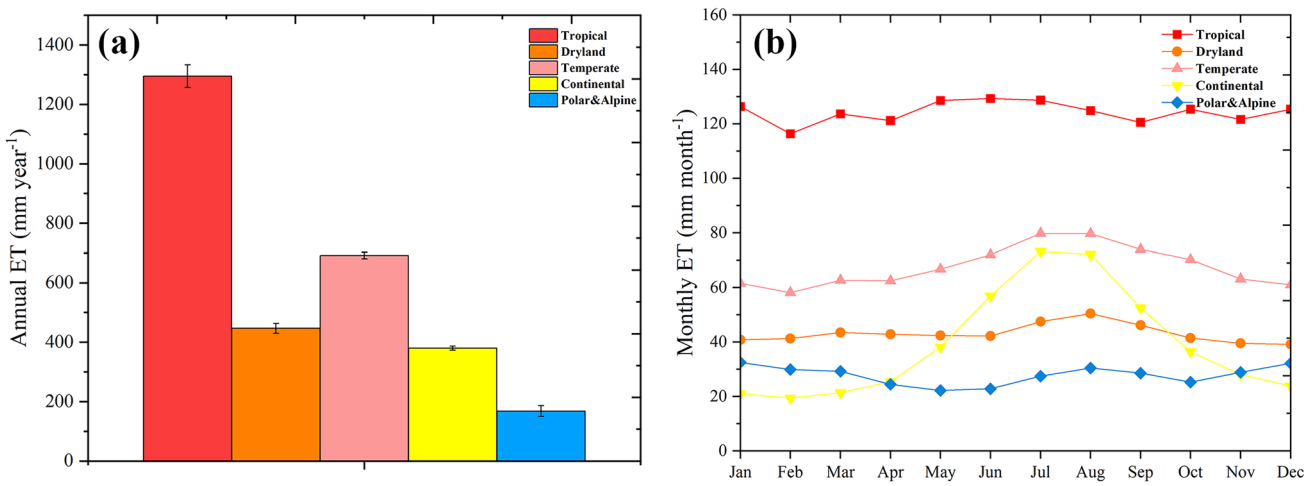

Fig. 11 **a** Muti-year annual mean and **b** seasonal cycle of ET_{AWB}, in the tropical zone, dryland zone, temperate zone, continental zone, and polar-alpine zone during 1983–2020. The error bar in **a** represents the standard deviation of the annual ET values

data available since 2002, due to the availability of terrestrial water storage data from GRACE. For instance, recently published TWB-based ET estimates for global large river basins began in 2002 (Ma et al. 2024; Xiong et al. 2023).

It is known that ERA5 data also provides long-term global ET estimates from 1940 to the present, demonstrating relatively good performance (Fig. 5). However, it should be noted that ET and P in the ERA5 reanalysis are computed from physical schemes that are usually not fully connected to the assimilation-based atmospheric moisture budgets. Specifically, P and ET are calculated by a forecast model that is only initialized once with the assimilation model. While the vertically integrated horizontal moisture divergence relies on detailed information about the variation in wind and humidity. Such measurements are usually derived from radiosondes observations. Consequently, if the simulated rainfall does not agree with ground-based measurements, the representation of moisture advection in the model is not necessarily wrong. Incorrect evapotranspiration can be compensated by an overestimation of precipitation, while the atmospheric moisture budget remains reasonable (Figure S8). Previous research has indicated that the precipitation from ERA5 is overestimated in many regions globally (Lavers et al. 2022). Hence, the analysis increments lead to an imbalance in the atmospheric water budget. Cullather et al., (2000) have reported that P − E values from NCEP and ECMWF forecast fields are about 60% below those obtained from the atmospheric moisture budgets. Given this, the long-term ET estimated based on the AWB in this study using observations including precipitation and moisture convergence as much as possible to mitigate the imbalance between the net water flux (P-ET) and vertically integrated horizontal moisture convergence in ERA5. Nevertheless, despite the AWB approach providing a direct and simple method to estimate long-term global ET values globally, poor quality in the representation of the surface process by reanalysis induces uncertainties (Builes-Jaramillo and Poveda 2018; Takacs et al. 2016).

4.2 Limitations and outlook of the atmospheric water balance method

The study area significantly influences the applicability of the water balances, as demonstrated by our results. It is shown that the uncertainties of ET_{AWB} are larger in tropical regions, which may be attributed to the lack of closure in the AWB, despite selecting four precipitation datasets in this study. Previous studies have reported that the AWB is not well represented in either the satellite data or reanalysis over tropical ocean regions, particularly in high-precipitation areas such as the Intertropical Convergence Zone (ITCZ) (Park et al. 2013; Trenberth and Smith 2005). It is much easier to estimate the water balance over land because of the availability and relatively low uncertainty of river flow data (Builes-Jaramillo and Poveda 2018). Additionally, although the AWB approach can overcome the limitations of TWB estimates for ET at basin scales and over short periods, it remains largely constrained by the scarcity of actual measurements, such as precipitation and the transport of water vapor by winds (Deng et al. 2022; Ukhurebor et al. 2020). Precipitation, in particular, exhibits significant variance on small temporal and spatial scales that the current observed system cannot sample sufficiently (Bengtsson 2010). The largest differences between various precipitation data occurred in the Amazon and the Congo Basin, as well as the polar regions, while minimal differences are observed in temperate and continental regions. (Figure S2, Negrón Juárez et al. 2009). Because temperate and continental zones, including the United States, Europe, and East Asia, have denser rainfall gauges and radiosonde observations compared to tropical and polar regions (Kidd et al. 2017).

The differences in ET_{AWB} derived using moisture convergence and atmospheric water vapor from various reanalysis data are significant regardless of the precipitation data used, highlighting the critical importance of the accurate winds and specific humidity from reanalysis data for calculating the atmospheric water balance. In the present study, our results demonstrate that ERA5 exhibits superior performance, aligning with previous research that highlights its higher accuracy compared to other reanalysis datasets (He et al. 2021; Tarek et al. 2020). Errors and uncertainties among different reanalysis datasets can be attributed to shortcomings in interpolation algorithms and the parameterization of diverse hydro-meteorological processes within various reanalysis products (Takacs et al. 2016). Specifically, reanalysis-predicted wind speeds often exhibit significant uncertainties and bias when compared to measured winds (Gualtieri 2022; Rose and Apt 2016; Torralba et al. 2017; Wu et al. 2024). Previous studies have indicated that reanalysis data, especially ERA5, are sufficiently reliable for predicting wind resources in offshore and flat onshore locations, whereas uncertainties are more profound in mountainous and coastal regions (Gualtieri 2022). Therefore, the use of higher-resolution regional products is recommended in these areas.

5 Conclusions

In this study, global monthly ET over 1983–2020 was calculated using the atmospheric water balance method, which requires three variables including moisture convergence, atmospheric water vapor, and precipitation. Here, the former two variables were from three reanalysis datasets (ERA5, JRA55, MERRA2), while the last variable came from four observation-based datasets (CRU, GPCC, GPCP, MSWEP).

Validations against the ET_{TWB} of 56 river basins indicate that the accuracy of ET_{AWB} primarily depends on the reanalysis data employed. ET_{AWB} derived from ERA5 demonstrates notably higher accuracy compared to those from JRA55 and MERRA2, regardless of the precipitation dataset employed. The large errors in the latter two are attributed to biases in the calculation of atmospheric moisture convergence using JRA55 and MERRA2.

The four ET_{AWB} estimates using the moisture convergence and atmospheric water vapor from ERA5 only and four precipitation datasets were merged to produce an ensemble mean ET_{AWB} dataset. Validations against the ET_{TWB} suggest that ET_{AWB} is more accurate than GLEAM and SITH in depicting the magnitude of ET, but its skill in depicting ET trends remains inferior. The 38-year mean global-averaged ET value estimated by the AWB approach is 619 ± 8 mm year^{-1} (excluding Antarctica). Across the global land, ET_{AWB} increased significantly with a trend of 0.35 mm year^{-1} ($p < 0.01$) during the period from 1983 to 2020. This corresponds to a 2.1% increase in global land ET over the past 38 years. The interannual variability is extremely strong in tropical regions due to the influence of internal climate variability on atmospheric moisture convergence and precipitation. The AWB-based ET estimates provide a valuable complementary picture for understanding the global ET process. Nevertheless, future efforts should incorporate more accurate ground observations and advanced data assimilation algorithms to further improve the accuracy of ET_{AWB}.

Supplementary Information The online version contains supplementary material available at https://doi.org/10.1007/s00382-024-07536-0.

Acknowledgements This work was supported by the National Science Foundation of China (42271029; 42171019), the Natural Science Foundation of Gansu Province (23JRRA1025), CAS Youth Innovation Promotion Association (2023059), the IGSNRR Kezhen-Bingwei Yongth Talents Program (2022RC003), and the Central Guidance for Local Science and Technology Development Fund Project (2024ZY0002). We also acknowledge the kind support by the Supercomputing Center of Lanzhou University.

Funding National Science Foundation of China, 42271029, Ning Ma, 42171019, Gaofeng Zhu, Gansu Postdoctoral Science Foundation, 23JRRA1025, Gaofeng Zhu, CAS Youth Innovation Promotion Association, 2023059, Ning Ma, IGSNRR Kezhen-Bingwei Yongth Talents Program, 2022RC003, Ning Ma, Central Guidance for Local Science and Technology Development Fund Project, 2024ZY0002, Ning Ma.

Data availability All data used in this study can be accessed from the website as follows: ERA5 (https://www.ecmwf.int/en/forecasts/dataset/ecmwf-reanalysis-v5); JRA55 (https://rda.ucar.edu/datasets/ds628.1/dataaccess/); MERRA2 (https://disc.gsfc.nasa.gov/datasets/M2IUNPANA_5.12.4/summary); GLEAM (https://www.gleam.eu/); SITHv2 (https://data.tpdc.ac.cn/zh-hans/data/a62f859d-c3ef-4b72-8ecd-6bd752d973271); ET_{TWB} (https://data.tpdc.ac.cn/en/data/e010cd0d-0881-4e7e-9d63-d36992750b04); GPCC (https://www.dwd.de/EN/ourservices/gpcc/gpcc.html); CRU (https://crudata.uea.ac.uk/cru/data/hrg/cru_ts_4.06/); GPCP (https://disc.gsfc.nasa.gov/datasets/GPCPMON_3.2/summary?keywords=GPCP); MSWEP (https://www.gloh2o.org/mswep/). The ensemble mean of ET_{AWB} dataset (0.25°, 1983-2020) is available at https://doi.org/10.6084/m9.figshare.28031951.

Declarations

Conflict of interest The authors declared that they have no conflicts of interest to this work.

References

Agrawal Y, Kumar M, Ananthakrishnan S, Kumarapuram G (2022) Evapotranspiration modeling using different tree based ensembled machine learning algorithm. Water Resour Manage. https://doi.org/10.1007/s11269-022-03067-7

Allen RG, Pereira LS, Howell TA, Jensen ME (2011) Evapotranspiration information reporting: I. Factors governing measurement accuracy. Agric Water Manage. https://doi.org/10.1016/j.agwat.2010.12.015

Amani S, Shafizadeh-Moghadam H (2023) A review of machine learning models and influential factors for estimating evapotranspiration using remote sensing and ground-based data. Agric Water Manag. https://doi.org/10.1016/j.agwat.2023.108324

Beck HE, Wood EF, Pan M, Fisher CK, Miralles DG, Van Dijk AIJM, McVicar TR, Adler RF (2019) MSWep v2 global 3-hourly 0.1° precipitation: methodology and quantitative assessment. Bull Am Meteorol Soc. https://doi.org/10.1175/BAMS-D-17-0138.1

Bengtsson L (2010) The global atmospheric water cycle. Environ Res Lett. https://doi.org/10.1088/1748-9326/5/2/025002

Berrisford P, Kållberg P, Kobayashi S, Dee D, Uppala S, Simmons AJ, Poli P, Sato H (2011) Atmospheric conservation properties in ERA-Interim. Q J R Meteorol Soc 137(659):1381–1399. https://doi.org/10.1002/qj.864

Bosilovich M, Akella S, Coy L, Cullather R, Draper C, Gelaro R, Kovach R, Liu Q, Molod A, Norris P, Wargan K, Chao W, Reichle R, Takacs L, Vikhliaev Y, Bloom S, Collow A, Firth S, Labow G, Suarez M (2015) MERRA-2: initial evaluation of the climate. NASA Tech Rep Series on Global Model Data Assimilation 43:139

Builes-Jaramillo A, Poveda G (2018) Conjoint analysis of surface and atmospheric water balances in the Andes-Amazon system. Water Resour Res. https://doi.org/10.1029/2017WR021338

Cai X, Yang ZL, Xia Y, Huang M, Wei H, Leung LR, Ek MB (2014) Assessment of simulated water balance from Noah, Noah-MP, CLM, and VIC over CONUS using the NLDAS test bed. J Geophys Res. https://doi.org/10.1002/2014JD022113

Chu H, Luo X, Ouyang Z, Chan WS, Dengel S, Biraud SC, Torn MS, Metzger S, Kumar J, Arain MA, Arkebauer TJ, Baldocchi D, Bernacchi C, Billesbach D, Black TA, Blanken PD, Bohrer G, Bracho R, Brown S, Zona D (2021) Representativeness of Eddy-Covariance flux footprints for areas surrounding AmeriFlux sites. Agric Forest Meteorol. https://doi.org/10.1016/j.agrformet.2021.108350

Cullather RI, Bromwich DH, Serreze MC (2000) The atmospheric hydrologie cycle over the arctic basin from reanalyses. part I: comparison with observations and previous studies. J Clim 13(5):923–937

Deng H, Zhang G, Liu C, Wu R, Chen J, Zhang Z, Qi M, Xiang X, Han B (2022) Assessment on the water vapor flux from atmospheric reanalysis data in the south china sea on 2019 summer. J Hydrometeorol. https://doi.org/10.1175/JHM-D-21-0210.1

Dominguez F, Kumar P, Liang XZ, Ting M (2006) Impact of atmospheric moisture storage on precipitation recycling. J Clim. https://doi.org/10.1175/JCLI3691.1

Fisher JB, Melton F, Middleton E, Hain C, Anderson M, Allen R, McCabe MF, Hook S, Baldocchi D, Townsend PA, Kilic A, Tu K, Miralles DD, Perret J, Lagouarde JP, Waliser D, Purdy AJ, French A, Schimel D, Wood EF (2017) The future of evapotranspiration: global requirements for ecosystem functioning, carbon and climate feedbacks, agricultural management, and water resources. Water Resources Res. https://doi.org/10.1002/2016WR020175

Fisher JB, Lee B, Purdy AJ, Halverson GH, Dohlen MB, Cawse-Nicholson K, Wang A, Anderson RG, Aragon B, Arain MA, Baldocchi DD, Baker JM, Barral H, Bernacchi CJ, Bernhofer C, Biraud SC, Bohrer G, Brunsell N, Cappelaere B, Hook S (2020) ECOSTRESS: NASA's next generation mission to measure evapotranspiration from the international space station. Water Resources Res. https://doi.org/10.1029/2019WR026058

Foken T (2008) The energy balance closure problem: an overview. Ecol Appl. https://doi.org/10.1890/06-0922.1

Gelaro R, McCarty W, Suárez MJ, Todling R, Molod A, Takacs L, Randles CA, Darmenov A, Bosilovich MG, Reichle R, Wargan K, Coy L, Cullather R, Draper C, Akella S, Buchard V, Conaty A, da Silva AM, Gu W, Zhao B (2017) The modern-era retrospective analysis for research and applications, version 2 (MERRA-2). J Clim. https://doi.org/10.1175/JCLI-D-16-0758.1

Gualtieri G (2022) Analysing the uncertainties of reanalysis data used for wind resource assessment: a critical review. Renew Sustain Energy Rev. https://doi.org/10.1016/j.rser.2022.112741

Harris I, Osborn TJ, Jones P, Lister D (2020) Version 4 of the CRU TS monthly high-resolution gridded multivariate climate dataset. Scientific Data 7(1):1–18. https://doi.org/10.1038/s41597-020-0453-3

He Y, Wang K, Feng F (2021) Improvement of ERA5 over ERA-interim in simulating surface incident solar radiation throughout China. J Clim. https://doi.org/10.1175/JCLI-D-20-0300.1

Hersbach H, Bell B, Berrisford P, Hirahara S, Horányi A, Muñoz-Sabater J, Nicolas J, Peubey C, Radu R, Schepers D, Simmons A, Soci C, Abdalla S, Abellan X, Balsamo G, Bechtold P, Biavati G, Bidlot J, Bonavita M, Thépaut JN (2020) The ERA5 global reanalysis. Q J Royal Meteorol Soc. https://doi.org/10.1002/qj.3803

Huffman GJ, Adler RF, Behrangi A, Bolvin DT, Nelkin EJ, Guojun GU, Ehsani MR (2023) The new version 3.2 global precipitation climatology project (GPCP) monthly and daily precipitation products. J Clim. https://doi.org/10.1175/JCLI-D-23-0123.1

Jasechko S, Sharp ZD, Gibson JJ, Birks SJ, Yi Y, Fawcett PJ (2013) Terrestrial water fluxes dominated by transpiration. Nature. https://doi.org/10.1038/nature11983

Jia Y, Li C, Yang H, Yang W, Liu Z (2022) Assessments of three evapotranspiration products over China using extended triple collocation and water balance methods. J Hydrol. https://doi.org/10.1016/j.jhydrol.2022.128594

Jung M, Reichstein M, Ciais P, Seneviratne SI, Sheffield J, Goulden ML, Bonan G, Cescatti A, Chen J, De Jeu R, Dolman AJ, Eugster W, Gerten D, Gianelle D, Gobron N, Heinke J, Kimball J, Law BE, Montagnani L, Zhang K (2010) Recent decline in the global land evapotranspiration trend due to limited moisture supply. Nature. https://doi.org/10.1038/nature09396

Jung M, Reichstein M, Margolis HA, Cescatti A, Richardson AD, Arain MA, Arneth A, Bernhofer C, Bonal D, Chen J, Gianelle D, Gobron N, Kiely G, Kutsch W, Lasslop G, Law BE, Lindroth A, Merbold L, Montagnani L, Williams C (2011) Global patterns of land-atmosphere fluxes of carbon dioxide, latent heat, and sensible heat derived from eddy covariance, satellite, and meteorological observations. J Geophys Res: Biogeosci. https://doi.org/10.1029/2010JG001566

Jung M, Koirala S, Weber U, Ichii K, Gans F, Camps-Valls G, Papale D, Schwalm C, Tramontana G, Reichstein M (2019) The FLUXCOM ensemble of global land-atmosphere energy fluxes. Scientific Data. https://doi.org/10.1038/s41597-019-0076-8

Kalma JD, McVicar TR, McCabe MF (2008) Estimating land surface evaporation: a review of methods using remotely sensed surface temperature data. Surv Geophys 29(4–5):421–469. https://doi.org/10.1007/s10712-008-9037-z

Kidd C, Becker A, Huffman GJ, Muller CL, Joe P, Skofronick-Jackson G, Kirschbaum DB (2017) So, how much of the earth's surface is covered by rain gauges? Bull Am Meteor Soc. https://doi.org/10.1175/BAMS-D-14-00283.1

Kim S, Anabalón A, Sharma A (2021) An assessment of concurrency in evapotranspiration trends across multiple global datasets. J Hydrometeorol. https://doi.org/10.1175/JHM-D-20-0059.1

Kobayashi S, Ota Y, Harada Y, Ebita A, Moriya M, Onoda H, Onogi K, Kamahori H, Kobayashi C, Endo H, Miyaoka K, Kiyotoshi T (2015) The JRA-55 reanalysis: general specifications and basic characteristics. J Meteorol Soc Jpn. https://doi.org/10.2151/jmsj.2015-001

Lavers DA, Simmons A, Vamborg F, Rodwell MJ (2022) An evaluation of ERA5 precipitation for climate monitoring. Q J R Meteorol Soc. https://doi.org/10.1002/qj.4351

Li J, Zhang G, Chen F, Peng X, Gan Y (2019) Evaluation of land surface subprocesses and their impacts on model performance with global flux data. J Adv Model Earth Syst. https://doi.org/10.1029/2018MS001606

Li J, Miao C, Wei W, Zhang G, Hua L, Chen Y, Wang X (2021) Evaluation of CMIP6 global climate models for simulating land surface energy and water fluxes during 1979–2014. J Adv Model Earth Syst. https://doi.org/10.1029/2021MS002515

Li J, Miao C, Zhang G, Fang YH, Shangguan W, Niu GY (2022) Global evaluation of the Noah-MP land surface model and suggestions for selecting parameterization schemes. J Geophys Res: Atmospheres. https://doi.org/10.1029/2021JD035753

Liu SM, Xu ZW, Zhu ZL, Jia ZZ, Zhu MJ (2013) Measurements of evapotranspiration from eddy-covariance systems and large aperture scintillometers in the Hai River, Basin China. J Hydrol. https://doi.org/10.1016/j.jhydrol.2013.02.025

Liu Y, Qiu G, Zhang H, Yang Y, Zhang Y, Wang Q, Zhao W, Jia L, Ji X, Xiong Y, Yan C, Ma N, Han S, Cui Y (2022) Shifting from homogeneous to heterogeneous surfaces in estimating terrestrial evapotranspiration: review and perspectives. Sci China Earth Sci. https://doi.org/10.1007/s11430-020-9834-y

Liu H, Xin X, Su Z, Zeng Y, Lian T, Li L, Yu S, Zhang H (2023) Intercomparison and evaluation of ten global ET products at site and basin scales. J Hydrol. https://doi.org/10.1016/j.jhydrol.2022.128887

Long D, Longuevergne L, Scanlon BR (2014) Uncertainty in evapotranspiration from land surface modeling, remote sensing, and GRACE satellites. Water Resour Res. https://doi.org/10.1002/2013WR014581

Ma N, Szilagyi J (2019) The CR of evaporation: a calibration-free diagnostic and benchmarking tool for large-scale terrestrial evapotranspiration modeling. Water Resour Res. https://doi.org/10.1029/2019WR024867

Ma N, Zhang Y (2022) Increasing Tibetan Plateau terrestrial evapotranspiration primarily driven by precipitation. Agric for Meteorol. https://doi.org/10.1016/j.agrformet.2022.108887

Ma N, Zhang Y, Szilagyi J, Guo Y, Zhai J, Gao H (2015) Evaluating the complementary relationship of evapotranspiration in the alpine steppe of the Tibetan Plateau. Water Resour Res. https://doi.org/10.1002/2014WR015493

Ma N, Szilagyi J, Zhang Y (2021) Calibration-free complementary relationship estimates terrestrial evapotranspiration globally. Water Resour Res. https://doi.org/10.1029/2021WR029691

Ma N, Zhang Y, Szilagyi J (2024) Water-balance-based evapotranspiration for 56 large river basins: a benchmarking dataset for global terrestrial evapotranspiration modeling. J Hydrol 630:130607. https://doi.org/10.1016/j.jhydrol.2024.130607

Martens B, Miralles DG, Lievens H, Van Der Schalie R, De Jeu RAM, Fernández-Prieto D, Beck HE, Dorigo WA, Verhoest NEC (2017) GLEAM v3: Satellite-based land evaporation and root-zone soil moisture. Geosci Model Develop 10(5):1903–1925. https://doi.org/10.5194/gmd-10-1903-2017

Melo DCD, Anache JAA, Borges VP, Miralles DG, Martens B, Fisher JB, Nóbrega RLB, Moreno A, Cabral OMR, Rodrigues TR, Bezerra B, Silva CMS, Neto AAM, Moura MSB, Marques TV, Campos S, Nogueira JS, Rosolem R, Souza RMS, Wendland E (2021) Are remote sensing evapotranspiration models reliable across south american ecoregions? Water Resources Res. https://doi.org/10.1029/2020WR028752

Miao H, Dong D, Huang G, Hu K, Tian Q, Gong Y (2020) Evaluation of Northern Hemisphere surface wind speed and wind power density in multiple reanalysis datasets. Energy. https://doi.org/10.1016/j.energy.2020.117382

Mo KC (2010) Interdecadal modulation of the impact of ENSO on precipitation and temperature over the United States. J Clim. https://doi.org/10.1175/2010JCLI3553.1

Mu Q, Heinsch FA, Zhao M, Running SW (2007) Development of a global evapotranspiration algorithm based on MODIS and global meteorology data. Remote Sens Environ. https://doi.org/10.1016/j.rse.2007.04.015

Negrón Juárez RI, Li W, Fernandes K, de Oliveira Cardoso A (2009) Comparison of precipitation data sets over the tropical South American and African continents. J Hydrometeorol. https://doi.org/10.1175/2008JHM1023.1

Oki T, Kanae S (2006) Global hydrological cycles and world water resources. Science. https://doi.org/10.1126/science.1128845

Oki T, Musiake K, Matsuyama H, Masuda K (1995) Global atmospheric water balance and runoff from large river basins. Hydrol Process. https://doi.org/10.1002/hyp.3360090513

Park H, Shin D, Yoo J (2013) Atmospheric water balance over oceanic regions as estimated from satellite, merged, and reanalysis data. J Geophys Res: Atmospheres. https://doi.org/10.1002/jgrd.50414

Pastorello G, Trotta C, Canfora E, Chu H, Christianson D, Cheah YW, Poindexter C, Chen J, Elbashandy A, Humphrey M, Isaac P, Polidori D, Ribeca A, van Ingen C, Zhang L, Amiro B, Ammann C, Arain MA, Ardö J, Papale D (2020) The FLUXNET2015 dataset and the ONEFlux processing pipeline for eddy covariance data. Scientific Data. https://doi.org/10.1038/s41597-020-0534-3

Ramillien G, Frappart F, Güntner A, Ngo-Duc T, Cazenave A, Laval K (2006) Time variations of the regional evapotranspiration rate from gravity recovery and climate experiment (GRACE) satellite gravimetry. Water Resour Res. https://doi.org/10.1029/2005WR004331

Ramon J, Lledó L, Torralba V, Soret A, Doblas-Reyes FJ (2019) What global reanalysis best represents near-surface winds? Q J R Meteorol Soc. https://doi.org/10.1002/qj.3616

Rasmusson EM (1968) Atmospheric water vapor transport anng the water banlance of North America. Mon Weather Rev. https://doi.org/10.1175/1520-0493(1968)096%3c0720:awvtat%3e2.0.co;2

Rodell M, Famiglietti JS, Chen J, Seneviratne SI, Viterbo P, Holl S, Wilson CR (2004) Basin scale estimates of evapotranspiration using GRACE and other observations. Geophys Res Lett. https://doi.org/10.1029/2004GL020873

Rose S, Apt J (2016) Quantifying sources of uncertainty in reanalysis derived wind speed. Renewable Energy. https://doi.org/10.1016/j.renene.2016.03.028

Salazar-Martínez D, Holwerda F, Holmes TRH, Yépez EA, Hain CR, Alvarado-Barrientos S, Ángeles-Pérez G, Arredondo-Moreno T, Delgado-Balbuena J, Figueroa-Espinoza B, Garatuza-Payán J, González del Castillo E, Rodríguez JC, Rojas-Robles NE, Uuh-Sonda JM, Vivoni ER (2022) Evaluation of remote sensing-based evapotranspiration products at low-latitude eddy covariance sites. J Hydrol. https://doi.org/10.1016/j.jhydrol.2022.127786

Seager R, Ting M, Held I, Kushnir Y, Lu J, Vecchi G, Huang HP, Harnik N, Leetmaa A, Lau NC, Li C, Velez J, Naik N (2007) Model projections of an imminent transition to a more arid climate in southwestern North America. Science. https://doi.org/10.1126/science.1139601

Shang S, Zhu G, Wei J, Li Y, Zhang K, Li R, Arnault JL, Zhang Z, Laux P, Yang Q, Donhg N, Gao L, Kunstmann H (2021) Associated atmospheric mechanisms for the increased cold season precipitation over the three-river headwaters region from the late 1980s. J Clim 34(19):8033–8046. https://doi.org/10.1175/JCLI-D-21-0077.1

Stopa JE (2018) Wind forcing calibration and wave hindcast comparison using multiple reanalysis and merged satellite wind datasets. Ocean Model. https://doi.org/10.1016/j.ocemod.2018.04.008

Sun S, Chen H, Wang G, Li J, Mu M, Yan G, Xu B, Huang J, Wang J, Zhang F, Zhu S (2016) Shift in potential evapotranspiration and its implications for dryness/wetness over Southwest China. J Geophys Res. https://doi.org/10.1002/2016JD025276

Sun S, Chen H, Sun G, Ju W, Wang G, Li X, Yan G, Gao C, Huang J, Zhang F, Zhu S, Hua W (2017) Attributing the changes in reference evapotranspiration in Southwestern China using a new separation method. J Hydrometeorol 18(3):777–798. https://doi.org/10.1175/JHM-D-16-0118.1

Sun S, Bi Z, Xiao J, Liu Y, Sun G, Ju W, Liu C, Mu M, Li J, Zhou Y, Li X, Liu Y, Chen H (2023) A global 5km monthly potential evapotranspiration dataset (1982–2015) estimated by the Shuttleworth-Wallace model. Earth System Sci Data. https://doi.org/10.5194/essd-15-4849-2023

Syed TH, Famiglietti JS, Chambers DP, Willis JK, Hilburn K (2010) Satellite-based global-ocean mass balance estimates of interannual variability and emerging trends in continental freshwater discharge. Proc Natl Acad Sci USA. https://doi.org/10.1073/pnas.1003292107

Szilagyi J, Ma N, Crago RD (2024) Revisiting the global distribution of the exponent of the power-function complementary relationship of terrestrial evaporation : insights from an isenthalpic index. J Hydrol 642(April):131864. https://doi.org/10.1016/j.jhydrol.2024.131864

Takacs LL, Suárez MJ, Todling R (2016) Maintaining atmospheric mass and water balance in reanalyses. Q J R Meteorol Soc. https://doi.org/10.1002/qj.2763

Tang R, Peng Z, Liu M, Li ZL, Jiang Y, Hu Y, Huang L, Wang Y, Wang J, Jia L, Zheng C, Zhang Y, Zhang K, Yao Y, Chen X, Xiong Y, Zeng Z, Fisher JB (2024) Spatial-temporal patterns of land surface evapotranspiration from global products. Remote Sens Environ 304:114066. https://doi.org/10.1016/j.rse.2024.114066

Tarek M, Brissette FP, Arsenault R (2020) Evaluation of the ERA5 reanalysis as a potential reference dataset for hydrological modelling over North America. Hydrol Earth Syst Sci. https://doi.org/10.5194/hess-24-2527-2020

Torralba V, Doblas-Reyes FJ, Gonzalez-Reviriego N (2017) Uncertainty in recent near-surface wind speed trends: a global reanalysis intercomparison. Environ Res Lett. https://doi.org/10.1088/1748-9326/aa8a58

Trenberth KE, Smith L (2005) The mass of the atmosphere: a constraint on global analyses. J Clim. https://doi.org/10.1175/JCLI-3299.1

Trenberth KE, Smith L, Qian T, Dai A, Fasullo J (2007) Estimates of the global water budget and its annual cycle using observational and model data. J Hydrometeorol. https://doi.org/10.1175/JHM600.1

Trenberth KE, Fasullo JT, Kiehl J (2009) Earth's global energy budget. Bull Am Meteor Soc. https://doi.org/10.1175/2008BAMS2634.1

Ukhurebor KE, Azi SO, Aigbe UO, Onyancha RB, Emegha JO (2020) Analyzing the uncertainties between reanalysis meteorological data and ground measured meteorological data. Measurement: J Int Measurement Confederation. https://doi.org/10.1016/j.measurement.2020.108110

Velpuri NM, Senay GB, Singh RK, Bohms S, Verdin JP (2013) A comprehensive evaluation of two MODIS evapotranspiration products over the conterminous United States: using point and gridded FLUXNET and water balance ET. Remote Sens Environ. https://doi.org/10.1016/j.rse.2013.07.013

Volk JM, Huntington J, Melton FS, Allen R, Anderson MC, Fisher JB, Kilic A, Senay G, Halverson G, Knipper K, Minor B, Pearson C, Wang T, Yang Y, Evett S, French AN, Jasoni R, Kustas W (2023) Development of a benchmark eddy flux evapotranspiration dataset for evaluation of satellite-driven evapotranspiration models over the CONUS. Agric for Meteorol. https://doi.org/10.1016/j.agrformet.2023.109307

Wang K, Dickinson RE (2012) A review of global terrestrial evapotranspiration: observation, modeling, climatology, and climatic variability. Rev Geophys. https://doi.org/10.1029/2011RG000373

Wild M, Folini D, Hakuba MZ, Schär C, Seneviratne SI, Kato S, Rutan D, Ammann C, Wood EF, König-Langlo G (2015) The energy balance over land and oceans: an assessment based on direct observations and CMIP5 climate models. Clim Dyn. https://doi.org/10.1007/s00382-014-2430-z

Wu L, Su H, Zeng X, Posselt DJ, Wong S, Chen S, Stoffelen A (2024) Uncertainty of atmospheric winds in three eidely used global reanalysis datasets. J Appl Meteorol Climatol. https://doi.org/10.1175/JAMC-D-22-0198.1

Xia Y, Mitchell K, Ek M, Sheffield J, Cosgrove B, Wood E, Luo L, Alonge C, Wei H, Meng J, Livneh B, Lettenmaier D, Koren V, Duan Q, Mo K, Fan Y, Mocko D (2012) Continental-scale water and energy flux analysis and validation for the North American land data assimilation system project phase 2 (NLDAS-2): 1. Intercomparison and application of model products. J Geophys Res Atmospheres. https://doi.org/10.1029/2011JD016048

Xiong J, Xu AL, Chandanpurkar HA, Famiglietti JS, Zhang C, Ghiggi G, Guo S, Pan Y, Vishwakarma BD (2023) ET-WB: water-balance-based estimations of terrestrial evaporation over global land and major global basins. Earth System Sci Data 15(10):4571–4597. https://doi.org/10.5194/essd-15-4571-2023

Yan Z, Wu B, Li T, Collins M, Clark R, Zhou T, Murphy J, Tan G (2020) Eastward shift and extension of ENSO-induced tropical precipitation anomalies under global warming. Sci Adv. https://doi.org/10.1126/sciadv.aax4177

Yang Y, Long D, Shang S (2013) Remote estimation of terrestrial evapotranspiration without using meteorological data. Geophys Res Lett. https://doi.org/10.1002/grl.50450

Yang YM, Park JH, An SI, Wang B, Luo X (2021) Mean sea surface temperature changes influence ENSO-related precipitation changes in the mid-latitudes. Nat Commun. https://doi.org/10.1038/s41467-021-21787-z

Yang Y, Roderick ML, Guo H, Miralles DG, Zhang L, Fatichi S, Luo X, Zhang Y, McVicar TR, Tu Z, Keenan TF, Fisher JB, Gan R, Zhang X, Piao S, Zhang B, Yang D (2023) Evapotranspiration on a greening earth. Nature Rev Earth Environ. https://doi.org/10.1038/s43017-023-00464-3

Yeh PJF, Famiglietti JS (2008) Regional terrestrial water storage change and evapotranspiration from terrestrial and atmospheric water balance computations. J Geophys Res Atmospheres 113(9):1–13. https://doi.org/10.1029/2007JD009045

Zeng Z, Wang T, Zhou F, Ciais P, Mao J, Shi X, Piao S (2014) A worldwide analysis of spatiotemporal changes in water balance-based evapotranspiration from 1982 to 2009. J Geophys Res. https://doi.org/10.1002/2013JD020941

Zeng Z, Piao S, Li LZX, Zhou L, Ciais P, Wang T, Li Y, Lian X, Wood EF, Friedlingstein P, Mao J, Estes LD, Myneni RB, Peng S, Shi X, Seneviratne SI, Wang Y (2017) Climate mitigation from vegetation biophysical feedbacks during the past three decades. Nat Clim Chang. https://doi.org/10.1038/nclimate3299

Zhang K, Zhu G, Ma J, Yang Y, Shang S, Gu C (2019) Parameter analysis and estimates for the MODIS evapotranspiration algorithm and multiscale verification. Water Resour Res. https://doi.org/10.1029/2018WR023485

Zhang K, Zhu G, Ma N, Chen H, Shang S (2022) Improvement of evapotranspiration simulation in a physically based ecohydrological model for the groundwater–soil–plant–atmosphere continuum. J Hydrol. https://doi.org/10.1016/j.jhydrol.2022.128440

Zhang Y, Li C, Chiew FHS, Post DA, Zhang X, Ma N, Tian J, Kong D, Ruby Leung L, Yu Q, Shi J, Liu C (2023) Southern Hemisphere dominates recent decline in global water availability. Science. https://doi.org/10.1126/science.adh0716

Zhang K, Chen H, Ma N, Shang S, Wang Y, Xu Q, Zhu G (2024) A global dataset of terrestrial evapotranspiration and soil moisture dynamics from 1982 to 2020. Scientific Data 11(1):1–17. https://doi.org/10.1038/s41597-024-03271-7

Zhao M, Geruo A, Liu Y, Konings AG (2022) Evapotranspiration frequently increases during droughts. Nature Clim Change. https://doi.org/10.1038/s41558-022-01505-3

Zheng C, Jia L, Hu G (2022) Global land surface evapotranspiration monitoring by ETMonitor model driven by multi-source satellite earth observations. J Hydrol. https://doi.org/10.1016/j.jhydrol.2022.128444

Zhu G, Zhang K, Chen H, Wang Y, Su Y, Zhang Y, Ma J (2019) Development and evaluation of a simple hydrologically based model for terrestrial evapotranspiration simulations. J Hydrol. https://doi.org/10.1016/j.jhydrol.2019.123928

Terms and Conditions

Springer Nature journal content, brought to you courtesy of Springer Nature Customer Service Center GmbH (“Springer Nature”).
Springer Nature supports a reasonable amount of sharing of research papers by authors, subscribers and authorised users (“Users”), for small-scale personal, non-commercial use provided that all copyright, trade and service marks and other proprietary notices are maintained. By accessing, sharing, receiving or otherwise using the Springer Nature journal content you agree to these terms of use (“Terms”). For these purposes, Springer Nature considers academic use (by researchers and students) to be non-commercial.
These Terms are supplementary and will apply in addition to any applicable website terms and conditions, a relevant site licence or a personal subscription. These Terms will prevail over any conflict or ambiguity with regards to the relevant terms, a site licence or a personal subscription (to the extent of the conflict or ambiguity only). For Creative Commons-licensed articles, the terms of the Creative Commons license used will apply.
We collect and use personal data to provide access to the Springer Nature journal content. We may also use these personal data internally within ResearchGate and Springer Nature and as agreed share it, in an anonymised way, for purposes of tracking, analysis and reporting. We will not otherwise disclose your personal data outside the ResearchGate or the Springer Nature group of companies unless we have your permission as detailed in the Privacy Policy.
While Users may use the Springer Nature journal content for small scale, personal non-commercial use, it is important to note that Users may not:

1. use such content for the purpose of providing other users with access on a regular or large scale basis or as a means to circumvent access control;
2. use such content where to do so would be considered a criminal or statutory offence in any jurisdiction, or gives rise to civil liability, or is otherwise unlawful;
3. falsely or misleadingly imply or suggest endorsement, approval , sponsorship, or association unless explicitly agreed to by Springer Nature in writing;
4. use bots or other automated methods to access the content or redirect messages
5. override any security feature or exclusionary protocol; or
6. share the content in order to create substitute for Springer Nature products or services or a systematic database of Springer Nature journal content.

In line with the restriction against commercial use, Springer Nature does not permit the creation of a product or service that creates revenue, royalties, rent or income from our content or its inclusion as part of a paid for service or for other commercial gain. Springer Nature journal content cannot be used for inter-library loans and librarians may not upload Springer Nature journal content on a large scale into their, or any other, institutional repository.
These terms of use are reviewed regularly and may be amended at any time. Springer Nature is not obligated to publish any information or content on this website and may remove it or features or functionality at our sole discretion, at any time with or without notice. Springer Nature may revoke this licence to you at any time and remove access to any copies of the Springer Nature journal content which have been saved.
To the fullest extent permitted by law, Springer Nature makes no warranties, representations or guarantees to Users, either express or implied with respect to the Springer nature journal content and all parties disclaim and waive any implied warranties or warranties imposed by law, including merchantability or fitness for any particular purpose.
Please note that these rights do not automatically extend to content, data or other material published by Springer Nature that may be licensed from third parties.
If you would like to use or distribute our Springer Nature journal content to a wider audience or on a regular basis or in any other manner not expressly permitted by these Terms, please contact Springer Nature at

onlineservice@springernature.com